Interaction of Phospholipase A_2 with Thioether Amide Containing Phospholipid Analogues†

Leigh A. Plesniak, Scott C. Boegeman, Brent W. Segelke, and Edward A. Dennis*

Department of Chemistry, 0601, University of California, San Diego, 9500 Gilman Drive, La Jolla, California 92093-0601

Received December 22, 1992; Revised Manuscript Received March 2, 1993

ABSTRACT: Transferred NOE experiments have been carried out on cobra venom (*Naja naja naja*) phospholipase A_2 (PLA_2) with substrate analogues which serve as potent inhibitors. 1-(Hexylthio)-2-(hexanoylamino)-1,2-dideoxy-*sn*-glycero-3-phosphoethanolamine (PE) and the corresponding phosphocholine analogue (PC) are water-soluble, short-chain, nonhydrolyzable substrate analogues which bind tightly to the enzyme. Because they are small compounds and monomeric in solution, NOEs develop inefficiently in the absence of enzyme. Thus, the PLA_2/inhibitor system is ideal for analyzing transferred NOEs. The experiments are carried out under conditions that are optimal for catalysis, pH 7.5 in the presence of 2 mM $CaCl_2$. The data show the inhibitor conformation in the catalytic site of cobra PLA_2 in solution. The effect of the thioether in the *sn*-1 chain on the chemical shift dispersion of the methylene protons allowed for chain-specific assignments and detailed conformational analysis. Both inhibitors adopt a PLA_2-bound conformation in which the end of the *sn*-2 chain is within 5 Å of the α-methylene of the *sn*-1 chain. In addition, intermolecular contact points between the inhibitor and the enzyme were identified by NOEs.

Cobra venom (*Naja naja naja*) phospholipase A_2 (PLA_2)[1] is a calcium-dependent enzyme that catalyzes the hydrolysis of the fatty acyl group at the *sn*-2 position of membrane phospholipids (Dennis, 1983). It is composed of a single polypeptide chain of 119 amino acids which contains 7 disulfide bonds. Overall, it is about 50% α-helical and heat stable. Several nonhydrolyzable substrate analogues for this enzyme, containing a thioether in the *sn*-1 chain and an amide in place of the *sn*-2 ester bond, bind in the catalytic site 10^3–10^4 times tighter than normal substrates (Yu et al., 1990; Yu & Dennis, 1991). We have now synthesized two analogues with short hydrophobic chains so that they would be monomeric in solution, a 1-thioether 2-amide phosphoethanolamine (PE) and a 1-thioether 2-amide phosphocholine (PC). We report herein the use of transferred NOE experiments to determine the conformation of these compounds when bound to the cobra PLA_2.

Transferred nuclear Overhauser enhancement (TRNOE) experiments are quite useful for probing substrate and inhibitor binding to enzymes. TRNOEs are negative NOEs that occur in systems where a small ligand is in fast exchange with a large macromolecule. The proper conditions for TRNOEs generally require a molar excess of ligand (Clore & Gronenborn, 1983). In the ligand's free state, dipolar relaxation is inefficient and NOEs develop slowly, but when the ligand is bound to a large macromolecule, dipolar relaxation is efficient and NOEs develop rapidly. Since the slow-tumbling condition is so much more efficient at dipolar relaxation than the fast-tumbling one, the bound ligand relaxation dominates, and its structural information is transferred to all ligands via the rapid exchange. Since an excess of ligand is generally required (sometimes up to 10× molar excess), the ligand resonances are easily observed in the presence of the less intense, broader protein signal. Finally, because the ligand signal is observed, the experiments are not constrained by the low pH and high enzyme concentrations that are optimum for obtaining high-resolution protein spectra. Thus, TRNOE experiments can be carried out under more biologically and kinetically relevant concentrations.

MATERIALS AND METHODS

Materials. Cobra venom PLA_2 (*N. naja naja*) was purified as described elsewhere (Hazlett & Dennis, 1985; Reynolds & Dennis, 1991) and was stored frozen at −20 °C. All organic solvents were purchased from Fisher, and deuterated NMR solvents were from Cambridge Isotope Laboratories. All other reagents were purchased from Aldrich and were reagent grade or better. Flash chromatography was performed with silica gel 60 (40 μm, Fisher). Aminopropyl solid-phase extraction sorbents were purchased from Varian either as Mega Bond Elute prepacked columns (60-mL column volume) or in bulk (Bondisil), preswollen (carboxymethyl)cellulose (CM52) was from Whatman, and nylon-66 filters (0.2 μm) were purchased from Rainin. Dry chloroform was prepared by extraction three times with water, followed by distillation over phosphorus pentoxide.

General Methods. Thin-layer chromatography (TLC) was carried out on Analtech silica gel GHLF 250-μm glass plates, and the compounds were visualized as previously described (Yu & Dennis, 1992). Before the samples were loaded, aminopropyl columns were cleaned by cycling through the solvents to be used on that particular column. The final concentrations of inhibitors were determined by phosphate assay as described previously (Yu & Dennis, 1992). For the

† This work was supported by NSF Grant DMB 88-17392 and NIH Grant GM 20501. The NMR spectrometer employed in these studies was purchased with funds provided by NIH Grant 1502-RR0342 and NSF Grant BBS 86-12359. Predoctoral fellowships were provided by NIH Training Grants 5 T32 GM 07313-1 (L.A.P. and B.W.S.) and 5 T32 CA 09523-06 (S.C.B.).

* To whom to address correspondence.

[1] Abbreviations: PLA_2, phospholipase A_2; PE and thioether amide PE, 1-(hexylthio)-2-(hexanoylamino)-1,2-dideoxy-*sn*-glycero-3-phosphoethanolamine; PC and thioether amide PC, 1-(hexylthio)-2-(hexanoylamino)-1,2-dideoxy-*sn*-glycero-3-phosphocholine; BPB, *p*-bromophenacyl bromide; MD, molecular dynamics; NOESY, nuclear Overhauser enhancement spectroscopy; TRNOE, transferred nuclear Overhauser enhancement; TOCSY, total correlated spectroscopy; FAB, fast atom bombardment; HRMS, high-resolution mass spectrometry; rmsd, root mean square deviation.

0006-2960/93/0432-5009$04.00/0

organic synthesis, ^{1}H-NMR spectra were obtained on an extensively modified Varian 360-MHz NMR spectrometer or a GE QE 300-MHz NMR spectrometer with chemical shifts recorded in parts per million (ppm) from tetramethylsilane (TMS).

Preparation of Amide Phospholipid Analogues. The syntheses of thioether amide analogues were reported previously (Bhatia & Hajdu, 1988). Recently, our group has published an alternative approach to the synthesis of these thioether amide phosphocholine analogues which allows one to easily change the length of the fatty acid at the *sn*-2 position (Yu & Dennis, 1992). By rearranging the sequence of the last three reactions, one can conveniently incorporate either a phosphocholine (PC) or a phosphoethanolamine (PE) headgroup into the structure. The synthesis below starts from the point of divergence of the previously reported synthesis (Yu & Dennis, 1992), detailing the last three steps.

1-(Hexylthio)-2-amino-1,2-dideoxy-3-[(2-bromoethyl)-phosphono]-sn-glycerol (**1**). 1-(Hexylthio)-2-(tritylamino)-1,2-dideoxy-3-[(2-bromoethyl)phosphono)-*sn*-glycerol (8.63 g, 13.9 mmol) was dissolved in neat trifluoroacetic acid (32 mL) and allowed to react at room temperature for 30 min. The trifluoroacetic acid was removed overnight in vacuo. The remaining residue was dissolved in 15 mL of chloroform/methanol (9:1) and applied to a flash silica gel column. The column was eluted with chloroform, followed by increasing amounts of methanol. The product eluted at chloroform/methanol (1:1) as the salt of trifluoroacetic acid to give an off-white solid (4.41 g, 84%). R_f was 0.88 in chloroform/methanol (4:1.5). ^{1}H-NMR ($CDCl_3$): δ 0.885 (t, 3 H), 1.354 (m, 6 H), 1.593 (t, 2 H), 2.562 (t, 2 H), 2.877 (br d, 2 H), 3.419 (br s, 1 H), 3.573 (br s, 2 H), 3.90–4.38 (br d, 4 H), 8.480 (br s, 3 H). HRMS (FAB, MH$^+$): m/z 378.0486; calculated for $C_{11}H_{26}NO_4PSBr$, 378.0504.

1-(Hexylthio)-2-(hexanoylamino)-1,2-dideoxy-3-[(2-bromoethyl)phosphono]-sn-glycerol (**2**). 1,1′-Carbonyldiimidazole (0.49 g, 3.0 mmol) was dissolved in 15 mL of dry chloroform. Triethylamine (50 μL, 0.36 mmol) and hexanoic acid (330 μL, 2.63 mmol) were added and allowed to react until gas evolution ceased (about 10 min). Compound **1** (0.68 g, 1.8 mmol) was dissolved in 9 mL of dry chloroform and added dropwise over 30 min. The reaction was left at room temperature overnight. After being quenched with methanol (1 mL), the solvent was removed to yield a yellow oil. The residue was dissolved in a minimum of chloroform/methanol (9:1) and distributed among three prepacked aminopropyl columns. The columns were washed with 1 column volume each of chloroform/methanol (9:1, 8:2, and 7:3), 2 volumes of ether with 2% acetic acid, and 1 volume of ether. The product eluted with chloroform/methanol/concentrated ammonium hydroxide (70:30:2). Residual acetic acid was removed overnight under vacuum to yield a light yellow oil (0.75 g, 87%). Exchangeable protons were removed with CD_3OD. ^{1}H-NMR ($CDCl_3/CD_3OD$, 1:1): δ 0.908 (m, 6 H), 1.333 (m, 10 H), 1.593 (m, 4 H), 2.217 (dt, 2 H), 2.575 (t, 2 H), 2.725 (m, 2 H), 3.541 (t, 2 H), 3.88–4.18 (m, 5 H).

1-(Hexylthio)-2-(hexanoylamino)-1,2-dideoxy-sn-glycero-3-phosphocholine (**3**). Compound **2** (0.92 g, 1.9 mmol) was allowed to react with aqueous trimethylamine as previously described (Dienbeck & Eibl, 1979). The volatile components were removed under vacuum. The residue was dissolved in chloroform and loaded onto a bulk aminopropyl column. The column was washed with chloroform, and the product eluted in chloroform/methanol (9:1) to give a partially purified product. This was dissolved in chloroform/methanol/water (65:25:1) and loaded onto a flash silica gel column. The product was eluted with chloroform/methanol/water (65:25:4.5) to give a clear oil. Solvent was removed under vacuum; the oil was dissolved in chloroform and passed through a 0.2-μm nylon-66 filter to remove particular matter. The yield was 0.51 g (58%). The product was stored in chloroform at −20 °C. R_f was 0.21 in chloroform/methanol/water (65:25:4). ^{1}H-NMR ($CDCl_3$): δ 0.884 (m, 6 H), 1.295 (m, 10 H), 1.581 (m, 4 H), 2.229 (q, 2 H), 2.552 (t, 2 H), 2.717 (m, 2 H), 3.427 (s, 9 H), 4.037 (m, 3 H), 4.195 (br d, 2 H), 4.493 (br s, 2 H), 7.524 (d, 1 H). HRMS (FAB, MH$^+$): m/z 455.2724; calculated for $C_{20}H_{44}N_2O_5PS$, 455.2709.

1-(Hexylthio)-2-(hexanoylamino)-1,2-dideoxy-sn-glycero-3-phosphoethanolamine (**4**). Compound **2** (0.52 g, 1.1 mmol) was allowed to react with ammonia as previously described (Dienbeck & Eibl, 1979). The volatile components were removed overnight under vacuum. The residue was dissolved in chloroform/methanol (3:1) and applied to a flash silica gel column. The column was washed with chloroform/methanol (65:25), followed by chloroform/methanol/water (65:25:0.25), and eluted with chloroform/methanol/water (65:25:0.5) to yield 0.18 g of partially purified product. This was further purified by using a (carboxymethyl)cellulose column as described previously (Comfurius & Zwaal, 1977). The product eluted between 9% and 14% methanol/chloroform. The final product, in methanol, was passed through a 0.2-μm nylon-66 filter to yield 0.11 g (24%). The product was stored in chloroform/methanol (4:1) at −20 °C. R_f was 0.57 in chloroform/methanol/water (65:25:4). Exchangeable protons were removed with CD_3OD. ^{1}H-NMR ($CDCl_3/CD_3OD$, 1:1): δ 0.910 (m, 6 H), 1.338 (m, 10 H), 1.591 (m, 4 H), 2.222 (dt, 2 H), 2.568 (t, 2 H), 2.714 (m, 2 H), 3.149 (br t, 2 H), 3.87–4.19 (m, 5 H). HRMS (FAB, MH$^+$): m/z 413.2255; calculated with $C_{17}H_{38}N_2O_5PS$, 413.2239.

Enzyme/Inhibitor NMR Sample Preparation. Cobra PLA_2 was concentrated and the buffer exchanged using a Centricon 3 (Amicon); the resulting protein was taken to dryness on a speed vac. Deuterium exchange was carried out two times. The protein was dried again and taken up in D_2O containing 2 mM $CaCl_2$ in the presence of thioether amide PE or thioether amide PC. All samples were adjusted to pH 7.5 (uncorrected for deuterium isotope effect) with DCl or NaOD and did not contain a buffer. Protein concentrations were 0.35 mM in a sample volume of 0.4 mL. The samples containing porcine pancreatic PLA_2 (Boehringer Mannheim) were prepared by desalting an ammonium chloride suspension on a Sephadex G-25 column and then were prepared in the same manner as the cobra enzyme.

p-Bromophenacyl Bromide/PLA_2 Sample Preparation. The covalent modification of cobra PLA_2 with *p*-bromophenacyl bromide (BPB) was carried out by combining 9 mg of cobra PLA_2 in 20 mL of water at pH 8.0 with 1.1 mL of 8 mM BPB in acetone to give final concentrations of 0.45 mg/mL PLA_2, 0.4 mM BPB, and 5.5% acetone (Roberts et al., 1977). The inactivation of the enzyme was followed with the pH-stat assay (Deems & Dennis, 1981) until less than 1% activity remained and then was quenched with acetic acid and hydrochloric acid to pH 3. The resulting mixture was purified over a Sephadex G-25 column. The NMR sample was prepared in the manner described above; however, NOESY spectra were run at pH 7.5 and 6.0 (uncorrected for deuterium) because of the increased solubility of the BPB-modified enzyme at the lower pH. Both pHs gave the same results.

NMR Spectra. For the binding studies, all spectra were obtained on a Bruker AMX 500-MHz NMR spectrometer

equipped with an Aspect 3000 process controller and collected in the phase-sensitive mode with TPPI phase cycling (Bodenhausen et al., 1980) at 40 °C. All data was processed on a Silicon Graphics workstation using Felix 2.0 (Hare Research, Inc.). The sweep width was 6944 Hz in both dimensions for all experiments. A continuous rf irradiation was applied during the recycle delay, and during the mixing time of the NOESY experiments, to saturate the residual HDO signal. DQF (double-quantum-filtered) COSY (Rance et al., 1983) were collected with 1.5-s relaxation delay and processed with sine-bell apodization in both dimensions. ROESY (rotating frame NOESY) experiments (Bax & Davis, 1985a) were carried out with mixing times ranging from 800 to 1200 ms. The TRNOE experiments were carried out with the standard NOESY (nuclear Overhauser effect spectroscopy) pulse sequence (Kumar et al., 1980). The TOCSY (total correlation spectroscopy) (Bax & Davis, 1985b) mixing time was 60 ms. The relaxation delay was 1.5 s. The NOESY and ROESY apodization used in t_2 was a Gaussian multiplier, with −5-Hz line broadening and a coefficient of 0.07. A squared skewed sine-bell apodization shifted 15° was used in t_1. The first point of each block in both dimensions was multiplied by 0.5 to reduce t_1 and t_2 ridges (Otting et al., 1986). The TOCSY was processed with a Gaussian multiplier using a coefficient of 0.2 in both dimensions and either −5-Hz (t_2) or −8-Hz (t_1) line broadening.

NOE Intensities. NOE cross-peak volumes were measured at 50-, 75-, 100-, 125-, 150-, and 175-ms NOESY spectra and normalized for the number of protons involved in the NOE (Macura & Ernst, 1980). The signal/noise ratios for the 50-ms mixing time experiments were inadequate to use for the distance constraints. For the PE, the 175-ms mixing time was also not employed for the distance approximations because of spin diffusion. Pseudoatoms were utilized for magnetically equivalent protons. The remaining NOE volumes were plotted against mixing time and assigned according to slope to the following classifications: strong, medium, weak, or very weak. After cross-peak volumes were classified, the distance approximations were calculated by assuming a NOE αr^{-6} relationship and standardizing against the nonequivalent geminal protons (F_a and F_b) with a distance of 1.8 Å. The initial NOE buildup for this proton pair remained linear throughout the range of mixing times employed in the calculations. The ranges for the distances were strong to a distance of 1.5 Å < r < 3.0 Å, medium 2.0 Å < r < 3.5 Å, weak 2.5 Å < r < 5.0 Å, and very weak 3.0 Å < r < 5.5 Å (Clore & Gronenborn, 1986; Bevilacqua et al., 1992).

Discover Model. We began our modeling studies by constructing an initial protein/substrate structure using the Biosym Insight II program package without the use of NMR data. The initial protein model of the enzyme was taken from the X-ray crystal structure of the cobra enzyme (Fremont et al., 1992). All water except the conserved catalytic site water molecule was removed. The substrate model was constructed, in a nonspecific conformation, and positioned at the catalytic site by interactive manipulation of torsions in the presence of a gridwise force field calculated for the catalytic site residues of the protein model. The resultant complex was then subjected to an iterative process of energy minimization and molecular dynamics (MD). Throughout the computational studies, the protein atoms and the catalytic site calcium atom were held fixed; all the substrate atoms were allowed to move freely with the exception of the *sn*-2 carbonyl oxygen, one of the phosphate oxygens, and the *sn*-2 carbonyl carbon. The *sn*-2 carbonyl oxygen and the phosphate oxygen were constrained to be within salt-bridging distance of the catalytic calcium, and the *sn*-2 carbonyl carbon was constrained to be within hydrogen-bonding distance of the catalytic water molecule (Dekker et al., 1991). The resultant model, chosen from 20 minimized structures, each from separate 10-ps simulations, had the lowest molecular mechanics energy while meeting the applied constraints.

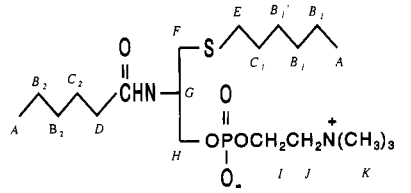

FIGURE 1: Chemical structure of the thioether amide PC with chemical shift assignments. The thioether amide PE lacks peak K.

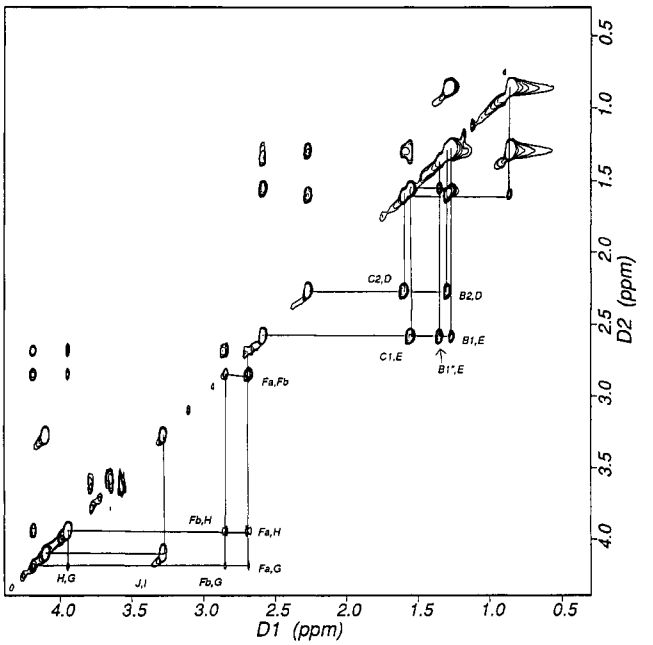

FIGURE 2: Section of a typical TOCSY of a 10:1 inhibitor/PLA_2 sample with a 60-ms mixing time. The methylenes of the *sn*-1 chain can be distinguished from the methylenes of the *sn*-2 chain. The sample contained 3.5 mM thioether amide PE and 0.35 mM PLA_2. In this experiment, 2 K points in t_2 and 400 points in t_1 were collected.

Table I: Chemical Shifts of Thioether Amide PE and PC (3.5 mM) in the Presence of PLA_2 (0.35 mM)

	chemical shift (ppm)			chemical shift (ppm)	
peak	PE	PC	peak	PE	PC
A	0.84	0.86	F_a	2.66	2.66
B_1	1.24	1.27	F_b	2.82	2.84
B_2	1.26	1.30	J	3.26	3.65
$B_{1'}$	1.33	1.34	I	4.08	4.29
C_1	1.53	1.56	H	3.92	3.94
C_2	1.57	1.61	G	4.16	4.19
D	2.26	2.26	K		3.20
E	2.56	2.58			

Structure Calculations. A model for the inhibitor was constructed from the substrate model above. The catalytic water was removed, and the model was subjected to energy minimization. Once the NOE data were translated into distance constraints, restrained molecular dynamics was employed to refine the model inhibitor's structure. However, another strategy was attempted which yielded lower energy conformations. Several families of inhibitor conformations were generated by applying the NOE distance constraints to

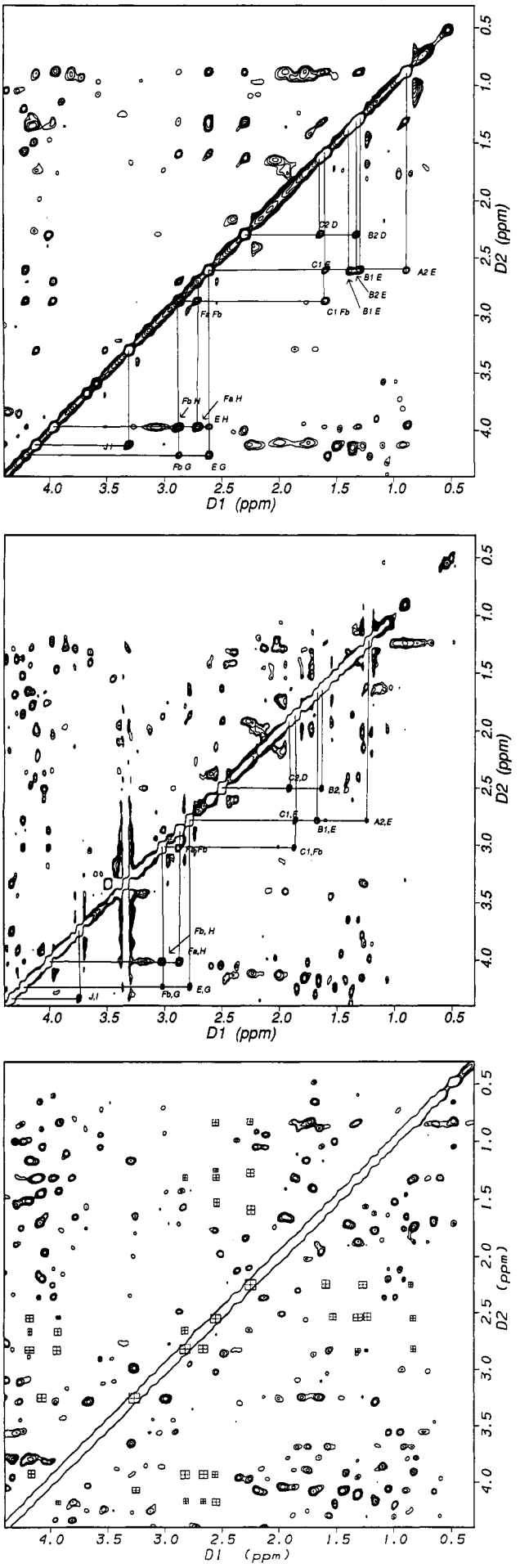

the thioether amide PE and the thioether amide PC in the absence of the protein. These conformational groups were the result of successive restrained molecular dynamics and energy minimizations. Several of these conformations, which had few violations of the NOE constraints, were docked to the enzyme and then subjected to further MD and energy minimizations with the use of the NOE constraints, as well as the intermolecular NOEs from the inhibitor to the protein and the two constraints that involve the active site calcium described above. Additionally, the calculations were carried out with the constraint of keeping the hydrogen bond between the His 48 and the amide proton on the inhibitor (Yu & Dennis, 1991). Violations to the constraints were treated with either a 100- or 5-kcal forcing potential. Both calculations gave similar results. The protein atoms and the active site calcium were again held fixed for all calculations.

RESULTS

Assignments and TRNOES. In order to assign the chemical shifts of the thioether amide PE and PC (Figure 1), a TOCSY (Figure 2) and a DQF COSY (data not shown) were carried out. Table I shows the chemical shifts of the thioether amide PE and PC in the presence of PLA_2. They were not significantly different in the absence of PLA_2. Since there is only one set of signals, which are broadened and of much greater intensity than the protein, the ligand is assumed to be in fast exchange between the free and bound forms on the chemical shift time scale. Because of the differing chemical structure of the *sn*-1 and *sn*-2 chains and their short length, the protons on the two fatty acid chains of the thioether amide PE and PC could be differentiated by their chemical shift, with the exception of the terminal methyl protons. For example, the thioether on the *sn*-1 chain shifts the α-methylene group (E) upfield from the α-methylene group on the *sn*-2 chain (D).

NOESY spectra were obtained with 5:1 and 10:1 ratios of inhibitor/PLA_2 for PE and 10:1 inhibitor/PLA_2 for PC. Typical NOESY spectra of PE and of PC are illustrated in Figure 3. Expanded regions of the NOESYs containing cross-peaks between the α-methylene protons of the two acyl chains and the rest of the methylenes in the chains are shown in panels A and B of Figure 4. The NOESY experiments were collected for mixing times ranging from 50 to 175 ms. The NOESY spectra gave cross-peaks that were of the same sign as the diagonal, indicating that the inhibitor is in the slow-tumbling extreme. The free inhibitor is in the fast-tumbling extreme; had the NOEs been from the free inhibitor, they would have had the opposite sign as the diagonal. Both intra- and intermolecular NOEs were observed.

In addition, control experiments were carried out with *p*-bromophenacyl bromide (BPB) inactivated enzyme with thioether amide PE, where the active site histidine is modified by BPB and blocks substrate binding (Roberts et al., 1977). The experiments showed evidence supporting the expected reduced binding affinity. There were no cross-peaks which exhibited rigid structure in the inhibitor or any long-range NOEs indicative of structure. An expanded region of this spectrum is shown in Figure 4D. Additionally, the intermo-

FIGURE 3: Sections of typical 125-ms NOESY spectra of (A, top) 3.5 mM thioether amide PE and 0.35 mM PLA_2 and (B, middle) 3.5 mM PC and 0.35 mM PLA_2. The identified cross-peaks are intramolecular TRNOEs, which generally are of greater intensity than the enzyme intramolecular NOEs which can be seen in panel C (bottom) for 0.35 mM PLA_2 alone. Boxes indicate where some of the peaks in spectra A and B are lacking in spectrum C.

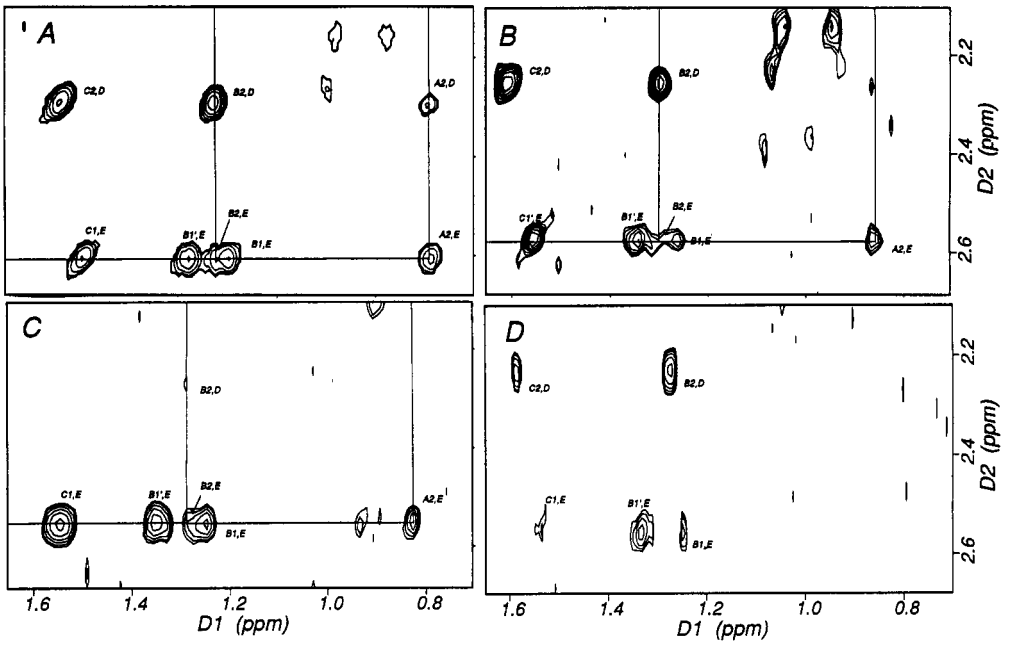

FIGURE 4: Sections of NOESY experiments expanded around the methylene cross-peaks to D and E, whereby the varying relative intensities of cross-peaks demonstrate different binding characteristics of the inhibitor: (A) PE/cobra PLA_2 (10:1), (B) PC/cobra PLA_2 (10:1), (C) PE/porcine pancreatic PLA_2 (5:1), and (D) PE/BPB-modified cobra PLA_2 (5:1). The NOESY spectra were obtained with a 125-ms mixing time except for (B), which used a 150-ms mixing time. The apodization was a sine bell in both dimensions, shifted 20° in t_1 and 30° in t_2.

lecular NOEs disappeared. These experiments demonstrate that active site binding is required for the observation of long-range NOESY cross-peaks and that they are not due to the formation of premicellar aggregates of lipid. Finally, ROESY experiments were done on the inhibitor in the absence of protein to check for evidence of the structure in the free state. The ROESY experiment was utilized for the free inhibitor because the nuclear Overhauser enhancement in molecules of this size is too small to measure with the NOESY. As expected, there was little evidence that the inhibitor possessed a rigid structure.

Additional TRNOE experiments were carried out with porcine pancreatic PLA_2, at a 5:1 PE inhibitor:PLA_2 ratio. An expanded region of this spectrum is shown in Figure 4C. This demonstrated binding but lacked some cross-peaks of the cobra PLA_2/PE complex. See Discussion. TRNOE experiments were also carried out on rattlesnake (*Crotalus atrox*) PLA_2, at a 10:1 PC inhibitor:PLA_2 ratio (data not shown). In contrast to the case with the pancreatic enzyme, *C. atrox* with a 10:1 PC inhibitor:PLA_2 ratio gave the same number of cross-peaks as the cobra enzyme.

NOE Buildups and Distance Constraints. The TRNOE experiments with 10:1 PE/PLA_2 gave a greater signal/noise ratio than the 5:1 sample. In addition, the NOE intensity buildup remained linear for longer mixing times with the 10:1 sample than with the 5:1 sample. For this reason, the 10:1 samples were used for distance approximations. The structure calculations of the PE and the PC were facilitated through the quantification of the NOEs through buildup curves which have been collected. Plots of NOE volume vs mixing time were carried out in order to categorize the cross-peaks as strong, medium, weak, and very weak. The plots of the PC's strong, medium, and weak NOEs are shown in Figure 5. NOEs that did not have sufficient signal/noise to obtain accurate volumes (not shown) were designated as very weak. NOEs that did not appear until longer mixing times and then built up quickly were assumed to be from spin diffusion and were not used for distance approximations. Although these constraints were not used, the distances in the calculated structures were generally within 6 Å. Although the signal/noise is good, one concern about distance approximations is the effect of exchange on NOE buildup rates (Campbell & Sykes, 1991). Because of this, the distance approximations were given wide ranges for the structure calculations.

The distance approximations were compared to the molecular model of the inhibitor bound to the catalytic site and then used to refine the model. There were a total of 25 NOEs for the PE and 27 for the PC. In both PC and PE, 5 of these were intermolecular NOEs to an aromatic residue on the protein. Ten of these NOEs were used in the dynamics calculations to generate structures of the bound conformation of the PE inhibitor. For the PC inhibitor, the NOE buildup curves showed greater linearity and divided more clearly into distance constraints so more constraints were used in the calculations. Fifteen of the NOEs were used in the calculations for the PC. In addition, constraints based on kinetic data (Yu & Dennis, 1991) and the porcine mutant complex structure (Thunnissen et al., 1990) were included in the dynamics and minimizations. These constraints employed both the phosphate oxygen and the carbonyl oxygen interactions with the calcium (3.2 Å $< r <$ 2.2 Å), as well as the active site histidine N-1 nitrogen constrained to the PE's amide proton to maintain linearity of the hydrogen bond (2.2 Å $< r <$ 1.5 Å), and were treated as NOE constraints. The NOE constraints and the resulting conformation for the PC inhibitor are shown in Figure 6A. Similar results were obtained for the PE inhibitor.

Structure Calculations. The structure calculations yielded several families of PE and PC structures. Each time an inhibitor was docked to the enzyme, a family of 20 structures was generated through repeated energy minimizations and restrained MD. Within a family, there was a high degree of agreement in the structures (about 0.5 Å rmsd over all atoms), with most of the deviation in the headgroup. This degree of agreement is the result of steric interference by the protein, which may prevent the inhibitor from finding its lower energy conformation. In order to find the lowest molecular mechanics energy conformation of the bound inhibitors, several docking experiments were carried out. The family of lowest energy

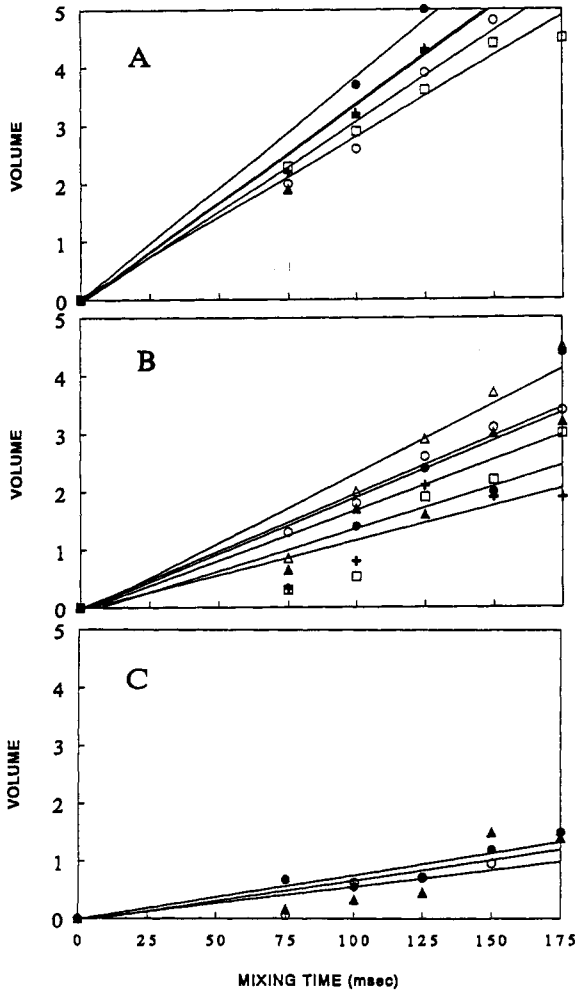

FIGURE 5: Graph of NOE volume vs mixing time for (A) strong NOEs F_a,H (▲), F_b,G (○), F_b,H (+), E,G (□), and I,J (●); (B) medium NOEs B_2,D (□), $B_{1'}$,E (▲), C_1,E (○), C_1,F_b (+), I,K (●), and C_2,D (△); and (C) weak NOEs A,E (○), B_1,E (▲), and F_a,G (●), from the PC/PLA_2 (10:1) data. The cross-peaks were divided into three categories on the basis of the magnitude of the slope and then grouped into distance approximations for the structure calculations.

PC structures had an average rmsd from the mean structure of 0.53 Å. The lowest energy conformations of PE and PC were similar. A comparison between the mean structures of the lowest energy families of PE and PC yielded an rmsd of 0.40 Å (excluding the ethanolamine and choline headgroups).

DISCUSSION

TRNOEs Represent Active Site-Bound Phospholipid. The thioether amide inhibitors are short-chain substrate analogs which mimic phospholipids. Replacing the ester with a nonhydrolyzable amide at the *sn*-2 position makes them potent inhibitors. The replacement of the *sn*-1 carbonyl with a thioether has two important benefits. The thioether increases the compound's binding affinity for cobra PLA_2. The thioether amide PE has an IC_{50} of 8 μM, and the PC has an IC_{50} of 90 μM (Boegeman and Dennis, unpublished results). The second benefit of the thioether is that it shifts the α-methylene signal on the *sn*-1 chain 0.3 ppm downfield of the signal from the *sn*-2 chain. All the *sn*-1 methylene resonances are shifted away from the *sn*-2 methylene proton signals, which allows the chains to be differentiated. This is important in determining contact points between the enzyme and the inhibitor, as well as its bound conformation. Because of the chemical shift dispersion of the methylene resonances, it is possible to determine which chain as well as which methylene on the inhibitor has an intermolecular NOE with PLA_2.

These short-chain inhibitors are monomeric in solution at concentrations below 10 mM. Therefore, structural studies with the protein should give information only about their bound state and should not be confused by structures resulting from formation of higher order aggregates such as micelles. The ROESY experiments with the inhibitors in the absence of protein confirmed this point. Without PLA_2, dipolar relaxation was not efficient enough to give any NOE cross-peaks until much longer mixing times (700 ms). Furthermore, even in the longer mixing time ROESY experiments there were no long-range NOEs indicative of an ordered structure, or an interaction between the *sn*-1 and *sn*-2 chain.

TRNOE experiments are a method for monitoring active site binding of the thioether amide inhibitors. The experiments show that a 5:1 and 10:1 molar ratio of inhibitor:PLA_2 at 40 °C in the presence of calcium gives strong intramolecular NOEs indicative of structure that are not present in experiments of monomeric lipid without protein. Because of the molar excess of ligand, these NOEs are picked out from the enzyme's signal with ease. We are certain the interaction is with the active site because the NOE intensities show a pH dependence coincident with the compounds' inhibition pH dependence which results in less tight binding at lower pH (data not shown) (Yu & Dennis, 1991). Additionally, in experiments where the enzyme's active site His 48 has been covalently modified with BPB, the experiments with thioether amide PE and PC show greatly reduced NOE intensities and are missing long-range NOEs altogether, including intermolecular NOEs which indicate reduced binding to PLA_2. Thus, micellization of the lipid by the protein is not responsible for the TRNOEs observed.

Conformation of Bound Phospholipid. Because we can distinguish between the methylenes on the *sn*-1 and *sn*-2 chains, and the methylenes along each chain, it is possible to determine their conformation with TRNOEs. The intramolecular NOEs of both the PE and PC indicate an interaction between the *sn*-1 and *sn*-2 chains. There is an NOE between B2 on the *sn*-2 and E on the *sn*-1 chain, which indicates that these protons are within 5 Å of each other. The strong overlap of the B_2,E cross-peak with B_1,E and $B_{1'}$,E did not allow for a clear volume measurement, so only a loose constraint for this NOE was used in the structure calculation. In addition, preliminary structure calculations for both PC and PE, as well as the buildup rate for the NOE intensity between peaks A and E, indicate that the cross-peak is from interactions between the *sn*-1 and *sn*-2 chains, rather than interaction along the chain. In the PE experiments, this interaction is more pronounced than with the PC.

In addition to the intramolecular TRNOEs, there were some intermolecular NOEs from the methylenes on the *sn*-2 chain to an aromatic residue on the protein (data not shown). On the basis of the model of the inhibitor complex derived without NOE constraints, this aromatic protein residue may be either Trp 19 or Phe 5.

Porcine Pancreatic PLA_2. The porcine pancreatic PLA_2, a PLA_2 with significant homology to the cobra enzyme (Davidson & Dennis, 1990), has a Phe 5 but does not have a Trp at position 19. Since the ^1H chemical shifts of the porcine enzyme protons have been assigned, a control TRNOE experiment was carried out to help determine the contact point between the inhibitor and this enzyme. In the experiments with the porcine enzyme and PE, the same intramolecular TRNOEs between the *sn*-1 and the *sn*-2 chain occurred, and

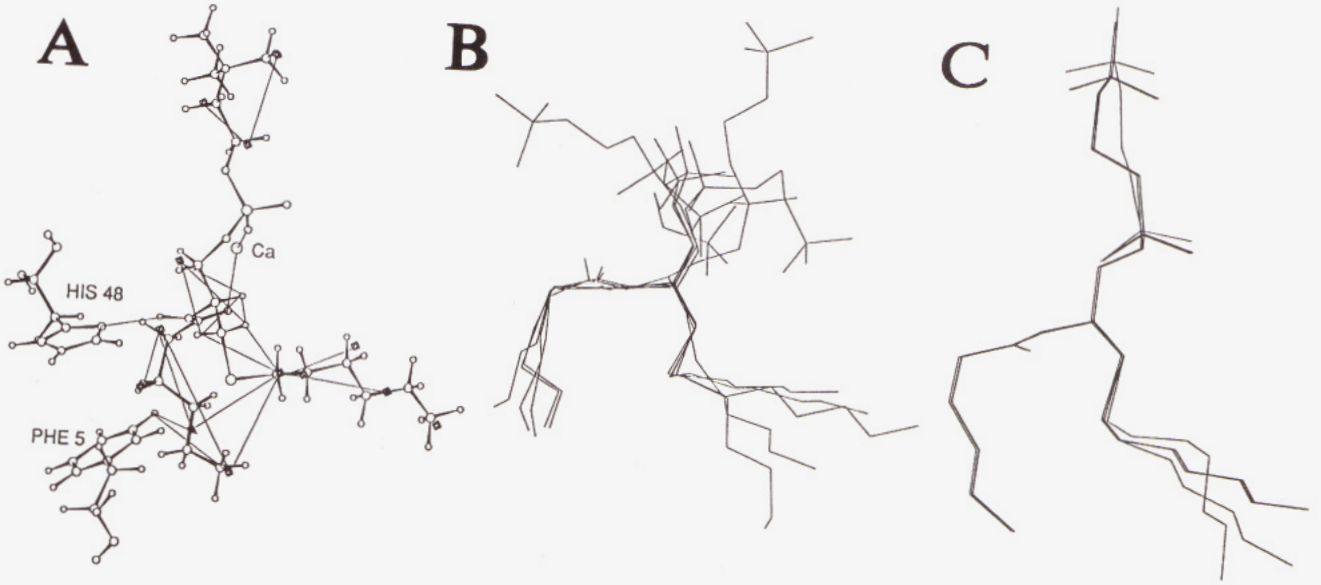

FIGURE 6: TRNOE-derived distance constraints (A) and conformations of the thioether amide PC (B) before docking to the cobra PLA_2 (C) and after. There is strong overlap of the bound calculated structures in the glycerol backbone and the *sn*-2 chain, but there is significant deviation in the *sn*-1 chain and the choline headgroup regions.

an intermolecular TRNOE with the *sn*-2 chain and an aromatic resonance that corresponded to the chemical shift of the protons of Phe 5 on the porcine enzyme was observed. This supports the conclusion that the Phe 5 on the cobra enzyme is within 2–5 Å of the *sn*-2 chain of the inhibitor. Our current efforts to assign the Trp proton resonances of the cobra enzyme indicate that the Trp resonances do not have the correct chemical shift to account for these intermolecular TRNOEs (Curto and Dennis, unpublished results). This also supports the assignment of the intermolecular TRNOEs as Phe 5.

Another interesting point about the experiment with the porcine enzyme is that there are differences in the mode of binding. The presence of the intermolecular TRNOEs confirms that binding occurs in the catalytic site; however, there is a noticeable lack of intramolecular TRNOEs involving the methylenes of the *sn*-2 chain (Figure 4C). This may be indicative of decreased rigidity in the bound state of the *sn*-2 chain of the inhibitor in the porcine pancreatic enzyme. It may be that Trp 19 in the cobra enzyme is important in anchoring this chain, which may help explain some of the differences in the kinetic behavior of the enzymes.

Model of the PLA_2/Inhibitor Complex. The initial model of the the inhibitor/PLA_2 complex was generated by visually docking an extended model of the inhibitor into the active site of the X-ray crystallographic structure of the enzyme. Undesirable steric interactions were removed by subsequent energy minimization and molecular dynamics calculations. The resultant minimized inhibitor conformation turns out to be similar in the headgroup and glycerol backbone region to that observed in the X-ray crystal structure of a mutant porcine pancreatic PLA_2 with a different amide bound (Thunnissen et al., 1990), although it was quite different in the acyl chains, probably due to their differing chemical structure and length of chains.

This model, which was in general agreement with the NOE data, was refined through the use of the distance constraints obtained from the TRNOE experiments. Several families of inhibitor structures consistent with the NMR data were generated in the absence of the protein (Figure 6B). The result of several restrained MD and minimization calculations was then docked to the enzyme and calculated with the same restrained dynamics and minimizations. The result of 15

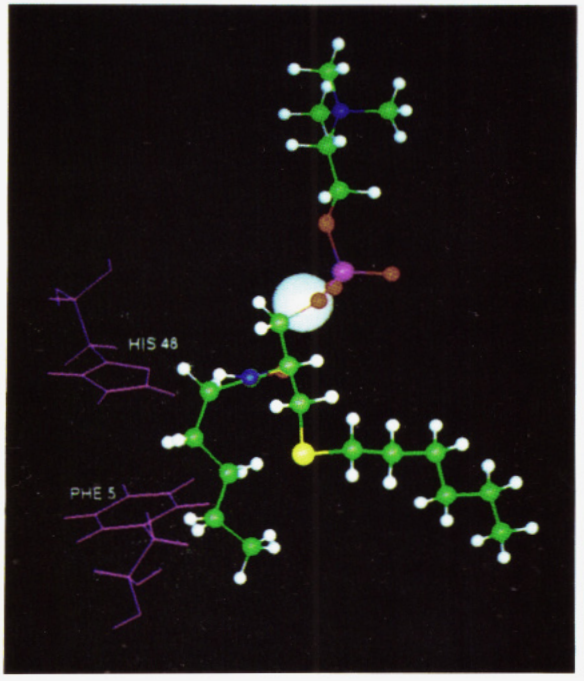

FIGURE 7: Average structure of the thioether amide PC bound to cobra PLA_2 in the presence of calcium (white sphere). The interactions with Phe 5 and His 48 on the enzyme are indicated.

calculations is shown in Figure 6C. This time, intermolecular constraints were included in the calculations. The resultant PC structure is shown in Figure 7. The headgroup has a conformation similar to that found in the crystal structure of the porcine mutant PLA_2 with the alkyl amide inhibitor complex; however, the chains differ significantly in conformation. The NMR restraints anchor the *sn*-2 chain into the active site through the intermolecular NOEs to the Phe 5. The interaction of the two chains and the intramolecular NOEs define the acyl chain conformation and glycerol backbone conformation quite well. However, NMR data do little to aid in the headgroup conformation. For this, the model presented relies heavily on the phosphate to calcium and calcium to carbonyl oxygen restraints, and on the force field used in the calculations. Each method in itself provides incomplete

information about the inhibitor. However, in combination they give a good picture of substrate binding. From Figure 6B, one can see that the *sn*-2 chain is ordered and the structures overlap well. However, the end of the *sn*-1 chain and the headgroup still exhibit disorder. This is most likely due to the lack of NMR-derived constraints rather than from mobility of the inhibitor and does not necessarily say anything about mobility in the chain.

The TRNOE data not only provide a picture of an inhibitor complex with PLA_2 but also have the potential to detect different characteristics of inhibitor binding. Figure 5 illustrates the differences in relative binding of the *sn*-1 and *sn*-2 chains. The thioether amide PC has lower intensities for the A_2,E, B_1,E, and B_2,E cross-peaks relative to $B_{1'}$,E and C_1,E. The decrease may indicate that the *sn*-1 and the *sn*-2 chains are not located as close to each other and that the *sn*-1 chain has a different conformation. It is also possible that the end of the *sn*-1 PC chain has more mobility than the end of the *sn*-1 chain on PE when bound. This is likely to be the case with the thioether amide PE when bound to the porcine pancreatic PLA_2. The B_2,D and C_2,D cross-peaks are absent; however, the TOCSY experiment (data not shown) confirms the chemical shifts, and the intermolecular NOE to Phe 5 is maintained. Since these cross-peaks are along the chain and must be in close proximity, the absence of the NOEs may indicate mobility in the chain. The BPB-modified PLA_2 has some association with the inhibitor because the observed TRNOE cross-peaks at short mixing times could only occur if the inhibitor was bound to PLA_2. The presence of any NOEs at this mixing time indicates that the inhibitor has a longer correlation time. However, the B_2,E and A,E cross-peaks which indicate an interaction between the *sn*-1 and *sn*-2 chains are absent. Additionally, all other intramolecular NOEs and intermolecular NOEs have disappeared. This suggests some binding or association but presumably not catalytic site binding.

The TRNOE data are the first experimental data in solution to probe inhibitor conformation in the catalytic site of cobra PLA_2. Previous work has been carried out with computer models which are not based on experimental data (Ortiz et al., 1992), and NMR work has been carried out on pancreatic PLA_2 in the presence of micelles (Thunnissen et al., 1990; Williams et al., 1989; Peters et al., 1992). The previous experiments were carried out with the primary intention of observing changes in the protein rather than observing the inhibitor's structure. The inhibitors previously used did not have the advantage of chemical shift dispersion of the methylenes that the thioether has created in our inhibitors, which has allowed for a more detailed structure determination. These previous experiments, which relied on observing the protein, must be run at lower pH (pH 3–4) to optimize the protein signal's resolution; however, both types of amide inhibitors bind with greatest affinity at neutral or slightly higher pH (Yu & Dennis, 1991, 1992). This is also the pH at which catalysis is optimal. The TRNOE experiments have the advantage in that they can be carried out at higher pH because the observed signal does not depend on the protein's line width. This results in a model for binding of the inhibitor in solution at the pH optimum of the enzyme.

ACKNOWLEDGMENT

We thank Dr. Lin Yu for his helpful suggestions regarding the synthesis of the inhibitors. We also thank Dr. Peter Wright of the Scripps Clinic and Research Foundation and Dr. Victor L. Hsu of UCSD for critical discussions. We acknowledge the support of the staff and facilities of the Southern California Regional Mass Spectrometry Facility, a unit of the UC Riverside Analytical Chemistry Instrumentation Facility.

REFERENCES

Bax, A., & Davis, D. G. (1985a) *J. Am. Chem. Soc. 107*, 2820.

Bax, A., & Davis, D. G. (1985b) *J. Magn. Reson. 63*, 207–213.

Bevilacqua, V. L., Kim, Y., & Prestegard, J. H. (1992) *Biochemistry 31*, 9339–9349.

Bhatia, S. K., & Hajdu, J. (1988) *Tetrahedron Lett. 29*, 31–34.

Bodenhausen, G., Vold, R. L., & Vold, R. R. (1980) *J. Magn. Reson. 37*, 93–106.

Campbell, A. P., & Sykes, B. D. (1991) *J. Magn. Reson. 93*, 77–92.

Clore, M. G., & Gronenborn, A. M. (1983) *J. Magn. Reson. 53*, 423–442.

Clore, M. G., & Gronenborn, A. M. (1986) *J. Mol. Biol. 190*, 259–267.

Comfurius, P., & Zwaal, R. F. A. (1977) *Biochim. Biophys. Acta 488*, 36–42.

Davidson, F. F., & Dennis, E. A. (1990) *J. Mol. Evol. 31*, 228–238.

Deems, R. A., & Dennis, E. A. (1981) *Methods Enzymol. 71*, 703–710.

Dekker, N., Peters, A. R., Slotboom, A. J., Boelens, R., Kaptein, R., Dijkman, R., & de Haas, G. (1991) *Eur. J. Biochem. 193*, 601–607.

Dennis, E. A. (1983) in *The Enzymes* (Boyer, P., Ed) 3rd ed., Vol. 16, pp 307–353, Academic Press, New York.

Dienbeck, W., & Eibl, H. (1979) *Chem. Phys. Lipids 24*, 237–244.

Fremont, D. H., Anderson, D., Wilson, I. A., Dennis, E. A., & Xuong, N.-H. (1993) *Proc. Natl. Acad. Sci. U.S.A. 90*, 342–346.

Hazlett, T. L., & Dennis, E. A. (1985) *Toxicon 23*, 457–466.

Kumar, A., Ernst, R. R., & Wuthrich, K. (1980) *Biochem. Biophys. Res. Commun. 95*, 1–6.

Macura, S., & Ernst, R. R. (1980) *Mol. Phys. 41*, 95–117.

Ortiz, A. R., Pisbarro, M. T., Gallego, J., & Gago, F. (1992) *Biochemistry 31*, 2887–2896.

Otting, G., Widmer, G., & Wuthrich, K. (1986) *J. Magn. Reson. 66*, 187–193.

Peters, A. P., Dekker, N., van den Berg, L., Boelens, R., Kaptein, R., Slotboom, A. J., de Haas, G. H. (1992) *Biochemistry 31*, 10024–10030.

Rance, M., Sorensen, O. W., Bodenhausen, G., Wagner, G., Ernst, R. R., & Wuthich, K. (1983) *Biochem. Biophys. Res. Commun. 117*, 479–485.

Reynolds, L. J., & Dennis, E. A. (1991) in *Methods in Enzymology* (Dennis, E. A., Ed.) Vol. 197, pp 359–365, Academic Press, Orlando, FL.

Roberts, M. F., Deems, R. A., Mincey, T. C., & Dennis, E. A. (1977) *J. Biol. Chem. 252*, 2405–2411.

Thunnissen, M. M., Ab, E., Kalk, K. H., Drenth, J., Dikstra, B. W., Kuipers, O. P., & Dijkman, R. (1990) *Nature 347*, 689–691.

Williams, M. P., Davis, P. D., Broadhurst, M. J., & Nixon, J. S. (1989) *Biochim. Biophys. Acta 997*, 9–14.

Yu, L., & Dennis, E. A. (1991) *Proc. Natl. Acad. Sci. U.S.A. 88*, 9325–9329.

Yu, L., & Dennis, E. A. (1992) *J. Am. Chem. Soc. 114*, 8757–8763.

Yu, L., Deems, R. A., Hajdu, J., & Dennis, E. A. (1990) *J. Biol. Chem. 265*, 2657–2664.